Mechanics of Advanced Composite Structures 4 (2017) 33-45

Semnan University

Mechanics of Advanced Composite Structures

journal homepage: http://MACS.journals.semnan.ac.ir

Improving Mechanical Properties of Nanocomposite-based Epoxy by High-impact Polystyrene and Multiwalled Carbon Nanotubes: Optimizing by a Mixture Design Approach

Y. Rostamiyan

Department of Mechanical Engineering, Sari branch, Islamic Azad University, Sari, Iran

PAPER INFO

Paper history:
Received 2016-09-03
Revised 2016-12-06
Accepted 2017-02-07

Keywords:
Carbon nanotube
Hybrid
Mechanical properties
Mixture design

ABSTRACT

In this study, the influence of the weight percentage of high impact polystyrene (HIP), the weight percentage of carbon nanotube (CNT), and hardener content on first– and second–mode damping properties of epoxy/HIPS/CNT hybrid composite was evaluated. Mixture design methodology was employed to generate mathematical models for predicting first– and second–mode damping behaviors of newly mentioned hybrid nanocomposite as function of physical factors and optimizing desired mechanical properties. The maximum and minimum values of first–mode damping occurred in run numbers 7 and 1, and were 3.71% and 1.64%, respectively. Moreover, maximum and minimum values of second–mode damping occurred in coded levels 9 and 1, with the values of 4.25% and 1.82%, respectively. Results of analysis of variance showed that input variables had a linear effect on both responses studied. Additionally, three component interactions X_1*X_2, X1*X_3, and X_2*X_3 affected first- and second-mode damping, as evidenced by their obtained P-values. Optimization results revealed that the highest values for first– and second mode damping were 3.53% and 4.11%, respectively. Coded values were 0.222 for HIPS; 0.301 for CNT; and 0.476 for hardener. Corresponding mixture components were: HIPS = 4.18 wt.%, CNT = 1.12 wt.%, and hardener = 25.75 per hundred resin (phr), respectively.

DOI: 10.22075/MACS.2017.1580.1076

1. Introduction

Polymer base composite materials are widely used the automotive, gas-turbine engine and aerospace industries due to their various advantages, such as economic efficiency, environment-friendly nature, and high chemical resistance with high stiffness and strength [1]. Considerable research have been done on polymeric composites in recent years, and nearly all focused on improving mechanical and thermal properties of these materials. In order to achieve this goal researchers reinforced thermoset or thermoplastic polymers with various materials [1]. Epoxy resin is one of the most important classes of polymer matrices because of its superior mechanical properties.

Epoxy resins are thermoset materials with good wetting ability, high activities, low viscosity, good fracture toughness, and excellent mechanical and thermal properties. Epoxy is the strongest polymeric material, with a tensile strength of 140 MPa [2]. But epoxy is naturally brittle because of its tight three-dimensional molecular network structure [3]. In order to address this problem, researchers were motivated to reinforce epoxy resin with various potential reinforcements. Reinforcements are generally divided in two groups: fibers, such as carbon fiber and glass fiber, and macro-, micro- or nanoparticles like nanosilica, carbon nanotubes, clay, nano TiO_2, etc. [4]. These

* Corresponding author. Tel.: +98-9111537063; Fax: +98-11-33033798

E-mail address: yasser.rostamiyan@iausari.ac.ir

additives have different effects on composite. For example, reinforcing with fiber distributes the stress throughout the restoration and improves the structure specifications of the composite by acting as a crack stopper [5-7]. Different types of fibers can be used as reinforcement. Glass fiber is more commonly used than other fibers. It can improve in–plane mechanical properties better than the others.

By investigating previous studies, we found that Panthapulakkal et al. [8] reinforced polypropylene composite with hemp and glass fiber and they found that thermal properties improved. Eronat et al. [2] evaluated the effects of glass fiber layering on flexural strength of microfill and hybrid composites. They showed that a glass–fiber layer of microfill and hybrid composites provided greater flexural strength. Bekyarova et al. [5] reinforced carbon nanotubes epoxy composite with carbon fiber and showed that the laminar strength was about 50 MPa, while Godara et al. [6] added CNTs into the carbon fibers and found that the viscosity of the epoxy matrix reinforced with different types of CNTs clearly depends on the type of CNT used. Also, a substantial increase (more than 80%) in fracture toughness was observed in mode 1 for pristine, multi–walled CNTs (MWCNTs) in combination with the epoxy resin.

Nanoparticles can be used as reinforcement also; they are easy and economical to fabricate and environmentally friendly [4]. Xu et al. [9] indicated that adding a low–weight percentage of nanoclay to fiber/epoxy composites improved their flexural strength by 38%. Gojny et al. [11] used 0.3 wt% MWCNT in glass fiber/epoxy composite as reinforcement and reported that its interlaminar shear strength significantly increased. Akbari et al. [13] added 5 phr (per hundred resin) liquid carboxyl-terminated butadiene acrylonitrile (CTBN) into the epoxy resin for toughening and 26% improvement in tensile strength was found. Ragosta et al. [13] showed that adding 10 wt% of nanosilica particles to the epoxy matrix improves its mechanical properties. Mirmohseni et al. [18] reinforced epoxy resin with 2.5 wt% organically modified clay and reported that its tensile modulus and strength, as well as its impact strength, increased compared with the neat epoxy. Becker et al. [12] showed that adding Nanomer I.30E nanoclay to epoxy resin improved its elastic modulus and fracture toughness. Zheng et al. [14] added 3 wt% of nanosilica to the epoxy matrix and reported that tensile strength and impact strength increased about 115% and 56%, respectively.

These higher mechanical property results encouraged researchers to combine two or more kinds of nano- or micro-particles as reinforcement, and hybrid nanocomposites were created [18]. Rostamiyan et al. [19] used HIPS in the thermoplastic phase and nanosilica as nanoreinforcement for epoxy resin and reported that a combination of HIPS and nanosilica increased the epoxy resin tensile and damping properties. Fereidoon at el. [16] reported that adding HIPS and CNTs as reinforcement improved tensile strength, as well as compressive and impact properties. Rostamiyan et al. [21] also filled epoxy resin with HIPS and nanoclay as a nanoreinforcement and found that tensile, impact and compression properties increased 60%, 64%, and 402%, respectively, compared with the compression properties of the neat one. Mirmohseni et al. [22] also showed that epoxy/ABS/nanoclay/Tio2 hybrid nanocomposite improved impact strength compared with neat epoxy. As mentioned previously, it is clear that there are various factors that affect final properties of hybrid nanocomposites, such as orientation of fibers and nanoreinforcement, thermoplastic phase, and hardener weight percentages. Controlling and optimizing these parameters helps control final mechanical properties and achieve desired specifications [23].

There are various mathematical methods for analyzing these parameters. One variation at time (OVAT) is a method for analyzing significant parameters in an experiment. This method analyzes only one variable at a time, but in most experimental studies there is more than one variable. Also, input variables depend on one another, and the effect of interactions is important and should be identified. Consequently, the OVAT method is not helpful in finding the real optimum point. Nonetheless, Leardi [24] claimed that 93% of the published papers in 2009 with general titles containing ‘‘optimization’’, ‘‘development’’, ‘‘improvement’’ or ‘‘effect of’’, employed the OVAT model. Moreover, predicting the nonlinear effect of a parameter is an important element that needs at least three points as a design-level parameter. These parameters directly increase the number of experiments for model prediction, which increases the costs and is also time-consuming.

As said previously, there are various mathematical methods for design of experiments (DOE) that can evaluate the nonlinear effect of input parameters or the effect of interaction between parameters. These methods optimize the results and help us find the best goal– related result. Response surface design (RSD) is the most frequently used statistical method for analyzing multiple factors, evaluating nonlinear effect of parameters and evaluating effects of interactions [25]. The mixture design approach is a subset of RSD. In this method, studied responses are made up of several components [26]. The independent factors of a mixture are proportions of the components and the sum of these proportions must be 1. Measured responses depend only on relative proportions rather than amounts. Another method is Taguchi design, which is a subset of design of experiments (DOE)

methods. This method uses orthogonal array, signal-to-noise (S/N) ratio and analyses of variance (ANOVA) for evaluating results and determining how input parameters affect the corresponding response. This method reduces the time and cost of carrying out the experiments.

In the current study, the effect of CNT as nanoreinforcement, HIPS as thermoplastic phase, and hardener content in the first- and second-mode damping properties of epoxy/HIPS/CNT hybrid nanocomposite was evaluated a using mixture-design approach. In addition, the effect of interaction between parameters was studied. Moreover, optimization was done in order to find the zone where both responses achieved their optimum value.

2. Experimental Details and Analysis

2.1. Details of materials

Difunctional bisphenol A (Epon 828) with an epoxide equivalent weight of 185-192 g/eqiv was selected as the epoxy resin utilized for this study; it was provided by Shell Chemicals Company. The curing agent was a nominally cycloaliphatic polyamine, Aradur-42, supplied by Huntsman Co. High impact polystyrene, used in this study as the thermoplastic phase, was purchased from Tabriz Petrochemical Co. MWCNTs used in this experiment were purchased from the Research Institute of Petroleum Industry (NIOC-RIPI) of Iran. The nanotubes have >95% purity and a maximum length of <30 μm and outer diameter of 10-20 nm. The selected solvent for this study, tetrahydrofuran (THF) with >99% purity, was provided by Merck Company (Germany).

2.2. Sample preparation

THF was used as an appropriate solvent for preparing a homogenous mixture to reinforce resin and also obtain comparable results. Liquid epoxy resin was poured into an adequate amount of THF solvent to ensure comparable situations with other neat epoxy samples; it was mixed for 30 minutes (min) on a magnetic stirrer. The mixture was poured into a vacuumed erlen, and the solvent evaporated completely within the vacuum created by a vacuum pump. Fig. 1 depicts the procedure. In the next step, a hardener with a stoichiometric ratio of 23 phr was added and mixed uniformly for about 15 min. It was then degassed by a vacuum pump. In next step, the mixture was poured in the silicon mold and cured for 24 hours (h) at room temperature, followed by post–curing from 50°C to 90°C every 2 h with a 20°C temperature enhancement interval and at 120°C for 2 h to ensure complete curing. To prepare the epoxy/HIPS/CNT samples, selected amounts of the reinforcements were dissolved in an adequate amount of similar solvent and mixed via magnetic stirrer for 30 min. In this study, the mixture was homogenized by ultrasonicating (Ultrasonic SONOPULS-HD3200) at 50% amplitude, 20 kHz, and pulsation - on for 10 seconds (s); off for 3 s - for 30 min. The required amount of epoxy resin for the neat epoxy samples was added to this mixture, following the same procedure; it was mixed mechanically at high speed for 2.5 h. Subsequently, the mixture was sonicated using the same procedure for 30 min. This protocol was followed as it was for the neat epoxy and, similarly, the stoichiometric ratio of hardener content varied for each hybrid sample.

2.3. Characterization

For the damping test, samples were prepared according to ASTM D256. The OMETRON Laser Doppler Vibrometer VH300 + shown in Fig. 2 measured the vibration. In this test, calculating natural frequencies and damping coefficients are based on Stochastic Subspace Identification-Data Driven (SSI-Data). Using this method, samples were considered cantilevered beam and were excited environmentally. All time-dependent responses were collected in a block Hankel matrix and then converted into individual past and future matrices. In order to make connections between responses, in the next step, the future matrix portrait on the past matrix created a projection matrix. By severance singular value decomposition (SVD) of the projection matrix, the observability matrix and Kalman states were calculated, and the collection of polar of system matrix was achieved. A TECNON scanning electron microscope (SEM) was used at 15KV to examine the fracture surface morphology of all prepared nanocomposite samples at their optimum concentration. These images were taken to evaluate nanoparticle dispersion in the resin and identify probable structural defects.

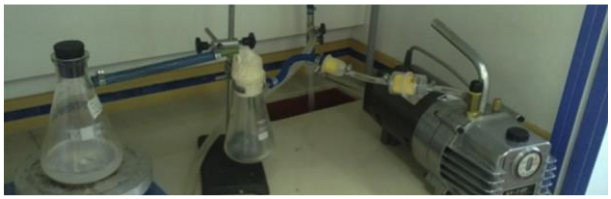

Figure 1: Mixing and solvent evaporation procedure under vacuum situation.

Figure 2. Vibration measured by the OMETRON VH300+ laser doppler vibrometer.

3. Experimental Design

Minitab statistical software (version 16.2.4) was used for analyzing and optimizing results in this study. A three–component, simplex–centroid mixture design was selected for designing the experiments. X_1, X_2, and X_3 were components of the mixture (X_1 = HIPS wt%, X_2 = CNT wt%, X_3 =hardener) content. The range of all components was between 0 and 1, and there were no constraints on the design space. Component proportions were expressed as fractions of the mixture, with a sum of 1 ($X_1 + X_2 + X_3 = 1$). Table 1 shows the experimental design and coded levels for three components as 10 combinations. These 10 design points consist of 3 single–ingredient treatments, 3 two–ingredient mixtures and 4 three–ingredient mixtures, as shown in Fig. 3. A total of 10 samples with different compositions (and no replicates) were prepared according to the simplex–centroid mixture configuration for a three-factor system (Table 1).

3.1. Statistical analysis and modeling of experimental data

In order to find the best model for fitting the experimental data, three models were selected: linear (1), quadratic (2), and special cubic (3).

$$Y = b_1X_1 + b_2X_2 + b_3X_3 \quad (1)$$

$$Y = b_1X_1 + b_2X_2 + b_3X_3 + b_1b_2X_1X_2 + b_1b3X_1X_3 + b_2b_3X_2X_3 \quad (2)$$

$$Y = b_1X_1 + b_2X_2 + b_3X_3 + b_1b_2X_1X_2 + b_1b_3X_1X_3 + b_2b_3X_2X_3 + b_1b_2b_3X_1X_2X_3 \quad (3)$$

Dependent and independent variables were fitted to these models, and residual plots were arranged to check its fitness. The best model should have high predicted R-squared, low standard deviation, and a low predicted sum of squares.

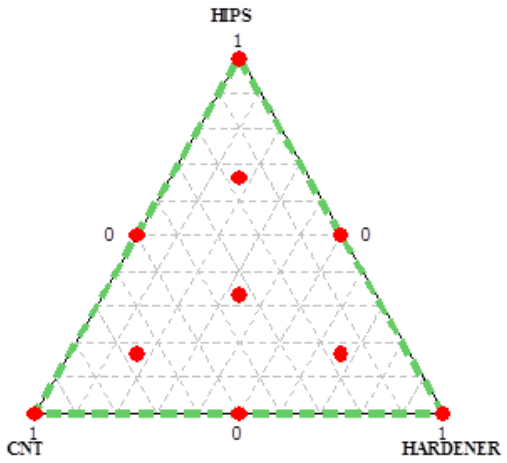

Figure 3. An overview of the simplex-shape mixture region for a three-component mixture.

According to these guides, the quadratic model was found to best represent the fitted response values. We determined the statistical significance of the model by analysis of variance (ANOVA) at 95%. The final quadratic model for three components is as follows:

$$H = \beta_1x_1 + \beta_2x_2 + \beta_3x_3 + \beta_{12}x_1x_2 + \beta_{13}x_1x_3 + \beta_{23}x_2x_3 \quad (4)$$

Where η is the predictive dependent variable (first and second damping), xis are the proportions of mixture components and βis are the equation coefficients that must be determined. Coded and actual levels of variables used to design the hybrid nanocomposite for this study are shown in Table 2, which indicates the weight percentage of CNT and HIPS; the hardener content is variable according to levels designed by model.

The most important goal of optimization studies is finding a combination of input variables that can maximize the desired responses simultaneously. To fulfill this, Minitab software's response optimization feature was used. Response optimization finds a combination of input variables that jointly optimize a set of responses by satisfying requirements for each response. In the first step, it calculates an individual desirability for each response based on a selected goal (maximize, minimize, or meet a target), and then it combines them to provide a measure of the composite, or overall, desirability of the multi-response system. Finally, response optimization employs a reduced gradient algorithm with multiple starting points that optimizes the composite desirability to determine optimal input variable settings.

4. Results and Discussion

As mentioned before, this study evaluated the damping property effects of incorporating HIPS in the thermoplastic phase and CNT as nanoreinforcement and hardener content into a diglycidyl ether of bisphenol A (DGEBA) type epoxy resin. These variables are shown in Table 3, as X_1, X_2, and X_3, respectively. Also, results collected from first– and second–mode damping tests are shown in Table 3, which provides clear evidence that the maximum and minimum values of first-mode damping 3.74% and 1.64%, respectively, occurring in run numbers 7 and 1. Additionally, the maximum and minimum values 4.25% and 1.82%, respectively, of second-mode damping occurred in coded levels 9 and 1. In the next stage, ANOVA was performed using Minitab software, with the following confidence levels: α = 0.01 and α = 0.05, which α = 0.01 accepts the terms with a probability value higher than 90% as effective, and α= 0.05 accepts those with a probability value higher than 95% as effective. ANOVA results in Table 4 are based on confidence levels α = 0.05, and effectiveness

of each variable should be evaluated according to its probability value (P-value). So, the terms with P≥95% (α≤0.05) are significant, and those with a P-value less than 95% (α≥0.05) are not effective and should be eliminated from final equations and analysis.

4.1. Analysis of variance

As seen in Table 4, both the first- and second-mode damping responses were well-fitted to the quadratic model with P-values of 0.013 and 0.002, respectively, and it is obvious that the fitness of second-mode damping was much better than that of first-mode damping, as evidenced by its probability value. Values of linear terms in Table 4 showed that each linear term (X_1, X_2, and, X_3) was effective on both responses according to their P-values, which were 0.014 and 0.003 for first- and second-mode damping, respectively. For first-mode damping response, it can be seen that three component interactions, X_1*X_2, X_1*X_3, and X_2*X_3 were significant with probability P= 98% and P>99% and P=95%, respectively. For the second mode of damping, the two component interactions were effective with P-value X_1*X_2= 0.017, X_1*X_3= 0.002 and X_2*X_3= 0.004. Hence, it can be concluded that the quadratic model showed the trends well and was suitable for this analysis. The interaction between parameters was more effective on second–mode damping compared with first–mode damping, according to the P–values obtained. Interaction between the HIPS and hardener content had the highest effect on first- and second-mode damping properties, as indicated by its probability value.

4.2. Regression coefficients and a fitting quadratic model

Regression coefficients for two corresponding responses are shown in Table 5. The coefficient of effective terms with P >95% are marked with one star, and those with P >99% are marked with two stars. The fitted regression quadratic models for first– and second–mode damping properties are as follows:

$$\eta = 1.564x_1 + 2.764x_2 + 2.862x_3 + 2.969x_1x_2 + 4.365x_1x_3 + 2.325x2x_3 \quad (5)$$

$$\eta = 1.775x_1 + 3.622x_2 + 2.516x_3 + 2.975x_1x_2 + 5.724x_2x_3 + 4.377x_2x_3 \quad (6)$$

The last column of Table 5 demonstrates the magnitude of index R^2, which is a measure of accuracy of results from the selected model. However, too more accurate estimation from the results can be provided if this value be closer to 100%. The R^2 values for first- and second-mode damping were about 0.94 and 0.98, respectively, so it seems that the regressors in the model explained all but about 6% of the total variability, indicating that the selected model provided a good estimation of responses. Also, based on the R^2 values, the model fit the data for the second-mode damping better than it did for first-mode damping.

Table 1: Mixture compositions and corresponding coded levels in the hybrid nanocomposite formulated with HIPS, CNT, and hardener in a three-component simplex centroid mixture design.

Formulation	Ingredient proportion		
	X_1 (HIPS)	X_2 (CNT)	X_3 (Hardener)
1	1.000	0.000	0.000
2	0.000	1.000	0.000
3	0.000	0.000	1.000
4	0.500	0.500	0.000
5	0.500	0.000	0.500
6	0.000	0.5000	0.500
7	0.333	0.333	0.333
8	0.667	0.167	0.167
9	0.167	0.667	0.167
10	0.167	0.167	0.667

Table 2: Actual and coded levels of the designed parameters.

HIPS content (wt.%)	CNT content (wt.%)	Hardener content (phr)	Level code
2	0.5	21	0.000
3.6	0.8	22.6	0.167
5.3	1.2	24.3	0.333
7	1.5	26	0.500
8.6	1.8	27.6	0.667
12	2.5	31	1.000

Table 3: Experimental design and obtained responses.

Std	Experimental factors (coded value)			First- and second-mode damping test results	
	HIPS (X_1) content	CNT (X_2) content	Hardener (X_3) content	1st Damping	2nd Damping
1	1.000	0.000	0.000	1.64	1.82
2	0.000	1.000	0.000	2.73	3.55
3	0.000	0.000	1.000	2.90	2.54
4	0.500	0.500	0.000	2.80	3.49
5	0.500	0.000	0.500	3.27	3.72
6	0.000	0.500	0.500	3.25	4.19
7	0.333	0.333	0.333	3.71	4.08
8	0.667	0.167	0.167	2.70	3.09
9	0.167	0.667	0.167	3.46	4.25
10	0.167	0.167	0.667	3.41	3.64

Table 4: Analysis of variance for all responses (component proportions).

	Source	DF	Seq SS	Adj SS	Adj MS	F	P
First-mode damping	Regression	5	2.92417	2.92417	0.584834	15.01	0.011
	Linear	2	1.25813	1.14947	0.574735	14.75	0.014
	Quadratic	3	1.66604	1.66604	0.555345	14.25	0.013
	X_1*X_2	1	0.43404	0.44618	0.446183	11.45	0.028
	X_1*X_3	1	0.95829	0.96455	0.964551	24.76	0.008
	X_2*X_3	1	0.27370	0.273705	0.273705	7.03	0.057
	Residual Error	4	0.15584	0.15584	0.038960	–	–
	Total	9	3.08001	–	–	–	–
Second-mode damping	Regression	5	5.20379	5.20379	1.04076	36.45	0.002
	Linear	2	2.16134	1.89935	0.94967	33.26	0.003
	Quadratic	3	3.04245	3.04245	1.01415	35.52	0.002
	X_1*X_2	1	0.42971	0.44804	0.44804	15.69	0.017
	X_1*X_3	1	1.64305	1.65851	1.65851	58.08	0.002
	X_2*X_3	1	0.96969	0.96969	0.96969	33.96	0.004
	Residual Error	4	0.11422	0.11422	0.02855	–	–
	Total	9	5.31801	–	–	–	–

4.3. Effect of main factors

Fig. 4 provides the main effect plot of input factors (HIPS wt.%, CNT wt%, and hardener content). Part 1 of Fig. 4 shows that increasing the HIPS portion had a reverse effect on both damping modes, so a lower wt% of this variable will have a better effect on studied responses. Part 2 of Fig. 4 shows that increasing the CNT wt.% first increased damping properties of both modes to a specific value before decreasing them slightly. However, the rate of decreasing the first mode of damping is greater compare to the first mode of damping. But the final value for both responses in this case was more than the first, so first- and second-mode damping generally increased the weight percentage of CNT. Part 3 of Fig. 4 shows that similar behavior can be observed for the effect of hardener content on first- and second-mode damping properties. Increasing the content of hardener increased the values obtained for two studied responses to a specific value and then decreased them. By comparing to the first mode of damping, the the second mode is greater.

Table 5: Regression coefficients and value of R2 for first-mode damping and second damping mode analysis of variance.

Responses	Coefficients						R^2
	β_1	β_2	β_3	β_{12}	β_{13}	β_{23}	
1st Damping	1.564*	2.764*	2.862*	2.969*	4.365**	2.325*	0.944
2nd Damping	1.775**	3.622**	2.516**	2.975*	5.724**	4.377**	0.978

*P-value more than 95%; **P-value more than 99%

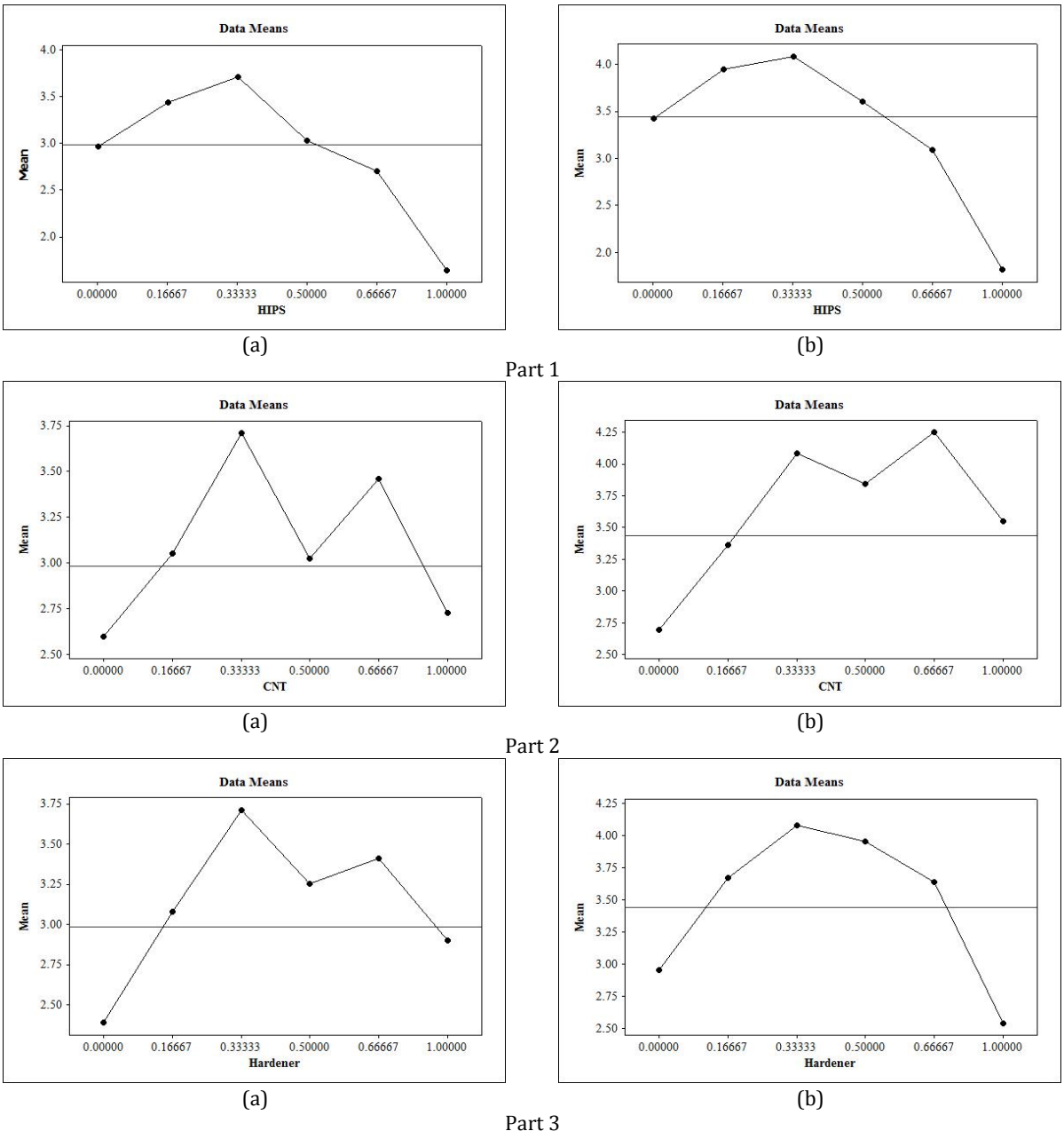

Figure 4. Effect of main factors of damping properties; Part 1) Main effect of HIPS on: (a) first–mode damping; (b) second-mode damping; Part 2) Main effect of CNT on: (a) first–mode damping; (b) second-mode damping; Part 3) Main effect of hardener on: (a) first–mode damping; (b) second-mode damping.

4.4. Normal probability plot of residual values

Fig. 5 presents the normal probability plot of residual values obtained from analysis of variance for first- and second-mode damping properties. These types of plots show whether a particular distribution fits the collected data and allows comparison of distinct sample distributions. Better fitness is indicated by proximity to the line; plotted points falling closer to the distribution line as well as closer to one another signify better fitness. Two parts of this figure describe that the fitted points for both studied responses were close to the fitted distribution line, but the second-mode damping points fell closer to the fitted distribution line and closer together compared with first-mode damping properties. So, normal distribution showed a better fitness for second–mode damping values.

4.5. Plots of residual versus fitted values

A plotting of residual versus fitted values for both damping modes is shown in the two parts of Fig. 6. It

can be seen from this figure that the residual values for both responses scattered on the display randomly, indicating that the model proposed was adequate and provided no reason to suspect any violation of the independent or constant variance assumption.

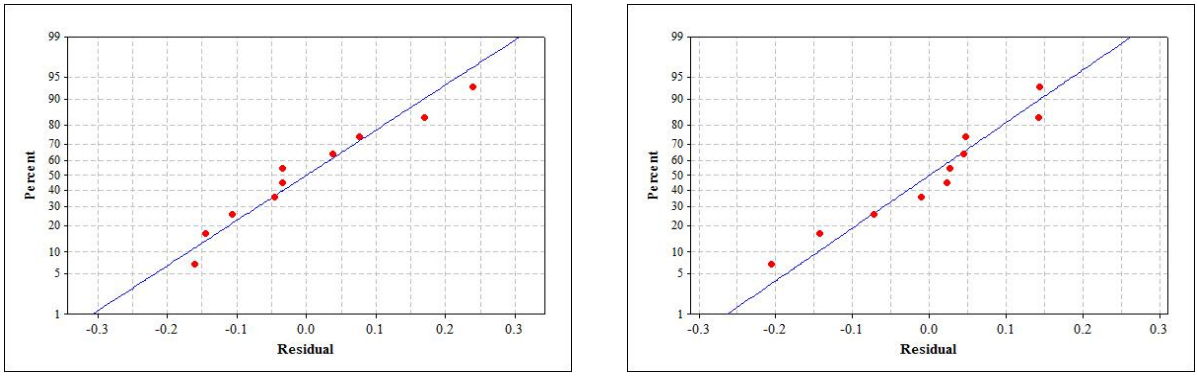

(a) (b)

Figure 5. Normal probability plot of residual values for: (a) first-mode damping; (b) second-mode damping.

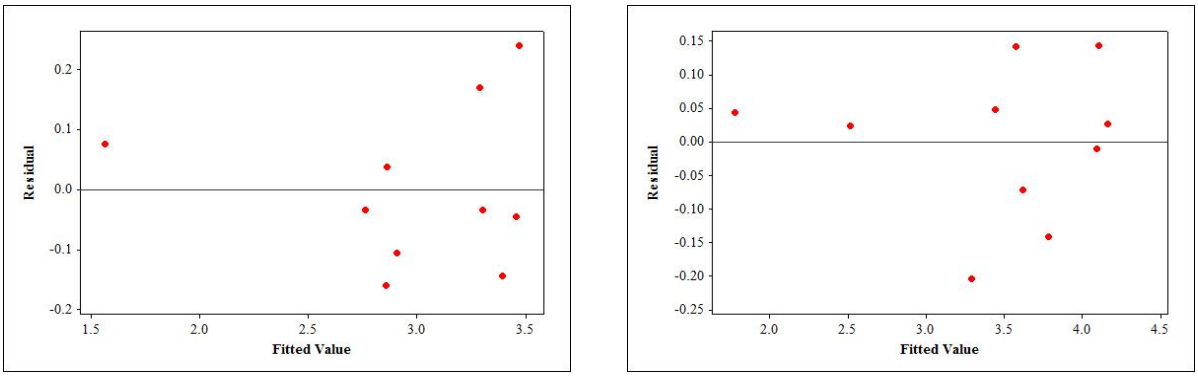

(a) (b)

Figure 6. Plot of residual versus fitted values for: (a) first-mode damping; (b) second-mode damping.

4.7. Response trace plots

Response trace plots show each mixture component's effect a specific response. Also called component–effect plots, their trace curves show the individual component's effect along an imaginary line connecting the reference blend on the vertex. Often the experimental region's centroid (center point) is chosen as the reference blend. Fig. 7 is a response-trace plot for two responses in this study. It can be concluded from the two parts of this figure that HIPS had a reverse effect on first- and second-mode damping, and increasing this parameter's value decreased both responses.

In addition, increasing the CNT weight percentage increased the magnitude of first- and second-mode damping before decreasing them slightly; however, first-mode damping changed at a higher rate and fell to a lower value than did second-mode damping. Finally, the hardener content affected both responses similarly. By increasing this variable's value, first- and second-mode damping magnitudes increased, and then both experienced a slight decrease, though second-mode damping experienced a higher decrease. These results are in agreement with results shown in Fig.4 and with main-effect plots discussed in previous sections.

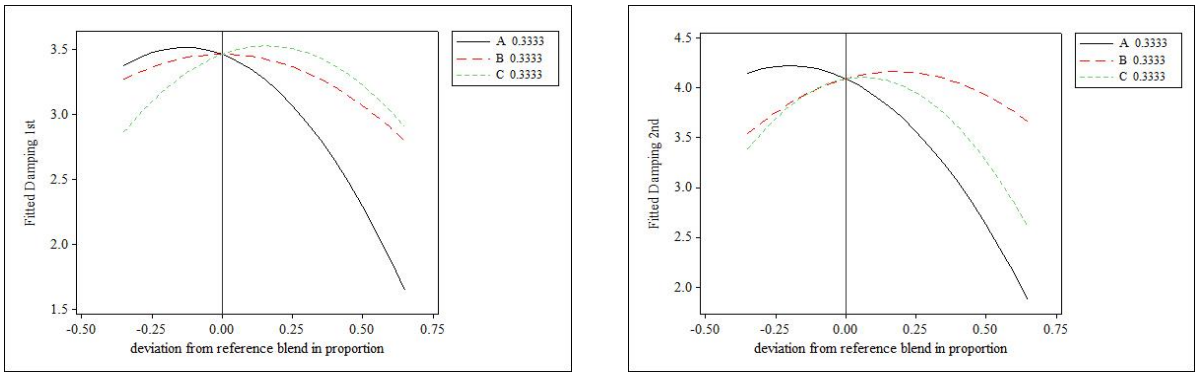

(a) (b)

Figure 7. Response trace plot for: (a) first-mode damping properties; (b) second-mode damping properties.

4.8. 2D contour plots

In this section, 2D contour plots have been employed to evaluate the effect of interactions of input variables on desired responses. A contour plot is a two–dimensional graphic technique that describes the effect on a response's values; in this study it describes the effects of combining mixture components. These contours involve different regions. A change in region color shows the trend of the response. So, darker regions indicate a higher magnitude of response, meaning that there was a greater effect on the specified response compared to lighter regions. Part (a) of Fig. 8 shows that increasing the HIPS and CNT values concurrently generally decreased the first–mode damping response. So, the interaction of X_1*X_2 was significant. In addition, increasing the value of two component interactions (X_1*X_3 and X_2*X_3) at the same time increased the value of first-mode damping. Moreover, as mentioned before, darker regions show higher values of first-mode damping properties (more than 3.5%) pertaining to designed test number 7. The maximum obtained value for the first-mode damping was 3.74%, belonging to this design level with the corresponding coded levels of HIPS = 0.333, CNT wt.% = 0.333, and hardener = 0.333, respectively. The minimum value obtained for first–mode damping was about 1.64%, which occurred in design level 1 with coded levels of X_1 = 1, X_2 = 0, and X_3 = 0, respectively. Part (b) of Fig. 8 shows a 2D contour plot for second-mode damping properties. As seen there, it is obvious that increasing two component interactions (X_1*X_2 and X_1*X_3) increased the second–mode damping, while increasing CNT and hardener magnitudes at the same time created a slight increase in the value of second-mode damping and decreased maximum values obtained for this response, as indicated by the darker region (more than 4%) and run numbers 6, 7, and 9. The maximum second–mode damping value was 4.25% for design level 9, with coded levels 0.16, 0.667, and 0.16 for X_1, X_2, and X_3, respectively. The minimum value obtained for second-mode damping was 1.82% for design level 1, with corresponding coded values of X_1 = 1, X_2 = 0, and X_3 = 0, respectively.

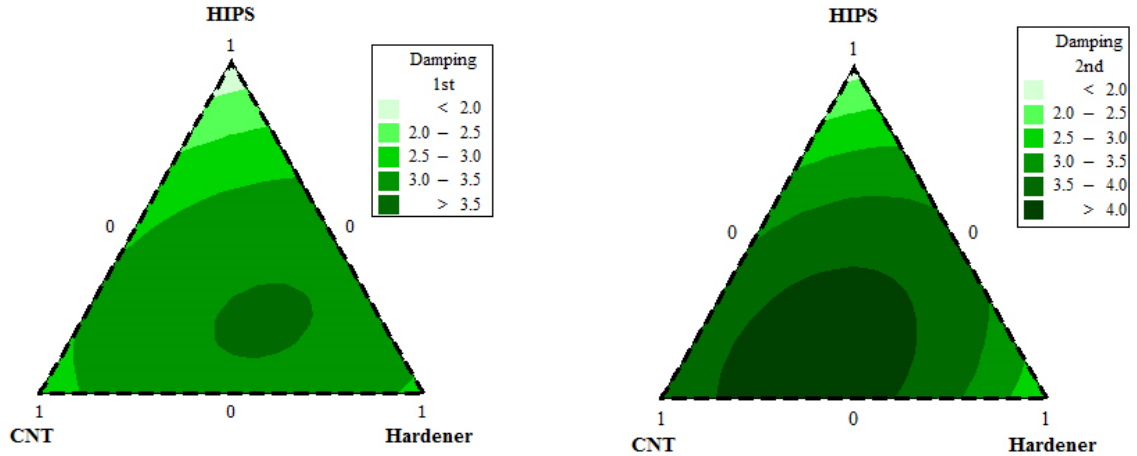

(a) (b)

Figure 8. 2D contour plots: (a) first-mode damping; (b) second-mode damping.

4.9. Response optimization

Fig. 9 is a response optimization plot for two interesting first- and second-mode damping properties responses. The purpose of generating this plot was to maximizing responses. So, values of target and allowable minimum responses were keyed into the software, and maximum achievable values for first- and second-mode damping properties, and corresponding coded values were returned. As seen in this figure, maximum achievable values for first- and second-mode damping were 3.53% and 4.11%, respectively.

This graph also shows individual and composite desirability values. Coded optimal magnitudes of mixture components were A = 0.222, B = 0.301, and C = 0.476, and corresponding actual values were HIPS = 4.18 wt%, CNT = 1.12 wt%, and hardener = 25.75 phr, respectively. Rostamiyan et al. [27] indicated that the optimum value for the first mode of damping was about 3.79%, which occurred in values of 4.87 w% for HIPS, 5.5 w% for nano silica and 29.25 phr for hardener. Also, they showed that optimum measured value for the second mode of damping that occurred in 5.05 w% for HIPS, 5.51w% for nano silica, and 29.56% phr for hardener.

These results clearly show that nanosilica as reinforcement yields better results than does CNT and gives us better damping properties. Rostamiyan et al. [28] used four different mechanisms of reinforcing for damping. Their results showed that epoxy with 5 wt% nanosilica in both the first- and second-damping modes reached their maximum value compared with other silica weight percentage loadings. And the values of 2 damping modes were increased up to 32% and 76% of neat value, respectively. In general, this study's results concur with those of earlier studies.

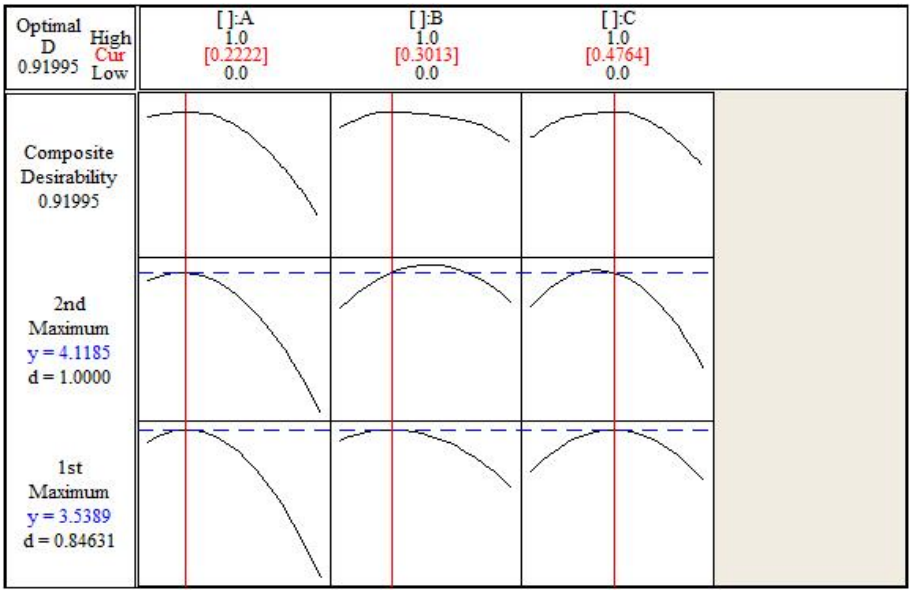

Figure 9. Response optimization plot for first- and second-mode damping properties.

4.10. Overlaid contour plots

Overlaid contour plots find the optimum region for both studied responses so the portions of a mixture component in this region can be calculated. Fig. 10 provides the overlaid contour plot for first– and second mode damping properties. The interference location of two diagrams in this figure is the region where both of the responses were at maximum with the same portions of mixture components. Coded levels of optimum points were 0.122, 0.512, and 0.364 phr for HIPS, CNT wt%, and hardener, respectively, and maximum responses values were 3.46% and 4.25% for first- and second-mode damping properties. It can be concluded that the results obtained from response optimization and the overlaid contour plot were in good agreement.

Finally, five samples were prepared and tested based on the optimum portions and values (3.38% and 4.22%) for first- and second-mode damping properties, respectively, so the actual maximum values for first- and second-mode damping properties were close to those derived theoretically.

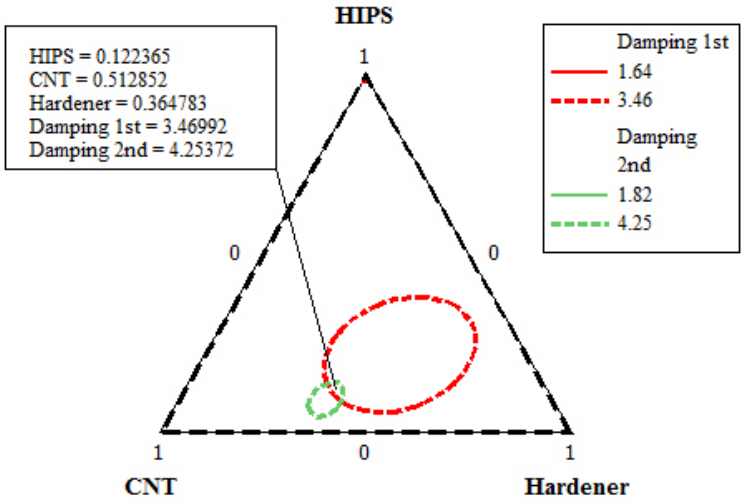

Figure 10. Overlaid counter plot for first- and second-damping modes.

4.11. SEM analysis

In order to have a better understanding of sample morphology, SEM analysis was done with optimum values of input variables. The micrograph cut surface of a damping specimen at the optimal amounts of HIPS, CNT, and hardener is shown in Fig. 11. In epoxy materials, cross-link density plays an important role in achieving good mechanical properties. Fig. 11(b) shows that good dispersion of high impact polystyrene and CNT nanoparticles with little agglomeration has obviously occurred. Moreover, phase separation of nano- and micro-particles in the epoxy matrix can be observed [29, 30].

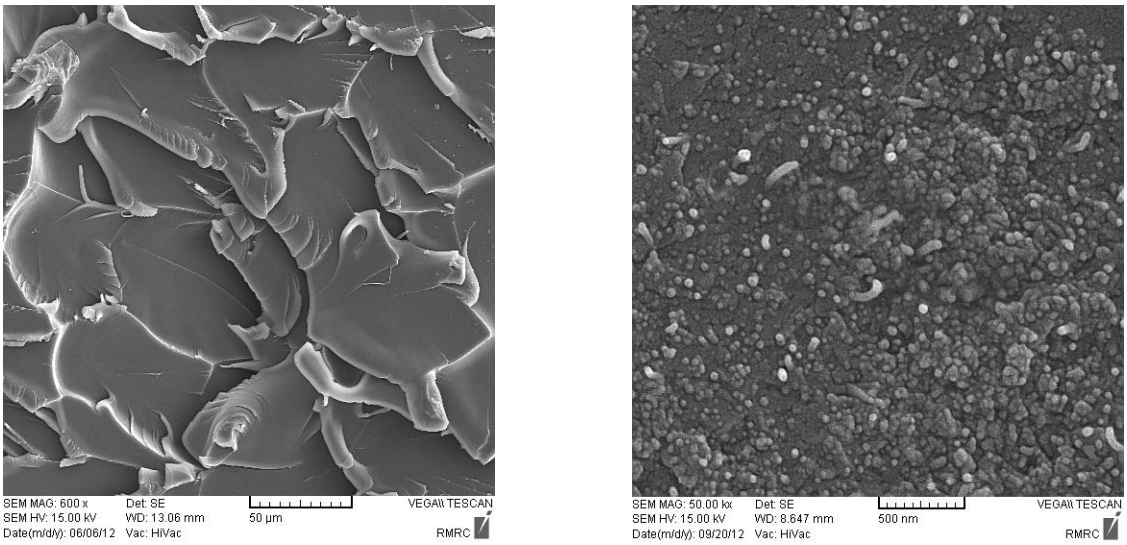

(a) (b)

Figure 11. Scanning electron micrographs of fracture surface for samples: (a) neat epoxy; (b) incorporating 4.18 wt.% HIPS and 1.12 wt.% CNT.

5. Conclusions

This study investigated the effect of weight percentage of HIPS and CNT, and of hardener content on first- and second-damping mode properties of epoxy/HIPS/CNT/hardener hybrid composite. Mixture design was used for analyzing results, and 10 samples were prepared and tested, based on variables portions. The results were fitted to the quadratic model. Analysis of variance was done using Minitab

software. ANOVA results showed that all input variables had a linear effect on both of the responses studied. Increasing the weight percentage of HIPS decreased two damping modes: increasing the weight percentage of CNT and the hardener content increased first- and second-mode damping to a certain value. It subsequently decreased, resulting in two interesting responses. Three component interactions (HIPS-CNT (X_1*X_2), HIPS-hardener (X_1*X_3) and CNT-hardener (X_2*X_3)) affected first and second modes of damping, due to their related probability values. Maximum values obtained from test were 3.71 and 4.25 for first and second mode of damping and minimum values of first and second mode of damping were 1.64 and 1.82 respectively.

In the next step, Minitab software enabled response optimization, yielding the following results: maximum value of first-mode damping: 3.51, maximum value of second mode damping: 4.22, coded values of mixture components were HIPS = 0.165, CNT = 0.434, and hardener = 0.400, with corresponding actual values of HIPS = 3.56 wt.%, CNT = 1.29 wt.%, and hardener = 24.58 phr. Finally, an overlaid contour plot was drawn based on minimum and maximum values of two mentioned responses, and the maximum region for both responses was obtained. Results of response optimization and the overlaid contour plot were in good agreement.

References

[1] Xu M, Hu J, Zou X, Liu M, Dong S, Zou Y. Mechanical and thermal enhancements of benzoxazine-based GF composite laminated by in situ reaction with carboxyl functionalized CNTs. *J Appl Polym Sci* 2013; 129(5): 2629-2637.

[2] Eronat N, Candan U, Turkun M. Effects of glass fiber layering on the flexural strength of microfill and hybrid composites. *J Esthetic Restorative Dentistry* 2009; 21(3): 171-178.

[3] Wu X, Wang Y, Xie L, Yu J, Liu F, Jiang P. Thermal and electrical properties of epoxy composites at high alumina loadings and various temperatures. *Iranian Polym J* 2013; 22(1): 61-73.

[4] LeBaron PC, Wang Z, Pinnavaia TJ, Polymer-layered silicate nanocomposites: an overview. *Appl Clay Sci* 1999; 15(1-2): 11-29.

[5] Vallittu PK. Flexural properties of acrylic resin polymers reinforced with unidirectional and woven glass fibers. *J Prosthetic Dentistry* 2009; 81(3): 318-326.

[6] Rostamiyan Y, Fereidoon A, Rezaeiashtiyani M, Mashhadzadeh AH, Salmankhani A. Experimental and optimizing flexural strength of epoxy-based nanocomposite: Effect of using nano silica and nano clay by using response surface design methodology. *Mater Des* 2015; 69: 96-104.

[7] Rostamiyan Y, Fereidoon A, Mashhadzadeh AH, Ashtiyani MR, Salmankhani A. Using response surface methodology for modeling and optimizing tensile and impact strength properties of fiber orientated quaternary hybrid nano composite. *Compos Part B: Eng* 2015; 69: 304-316.

[8] Panthapulakkal S, Sain M. Injection-molded short hemp fiber/glass fiber-reinforced polypropylene hybrid composites - Mechanical, water absorption and thermal properties. *J Appl Polym Sci* 2007; 103(4): 2432-2441.

[9] Bekyarova E, Thostenson ET, Yu A, Kim H, Gao J, Tang J. Multiscale carbon nanotube-carbon fiber reinforcement for advanced epoxy composites. *Langmuir* 2007; 23(7): 3970-3974.

[10] Godara A, Mezzo L, Luizi F, Warrier A, Lomov SV, van Vuure AW. Influence of carbon nanotube reinforcement on the processing and the mechanical behaviour of carbon fiber/epoxy composites. *Carbon* 2009; 47(12): 2914-2923.

[11] Xu Y, Hoa SV. Mechanical properties of carbon fiber reinforced epoxy/clay nanocomposites. *Compos Sci Technol* 2008; 68(3-4): 854-861.

[12] Gojny FH, Wichmann MHG, Fiedler B, Bauhofer W, Schulte K. Influence of nano-modification on the mechanical and electrical properties of conventional fibre-reinforced composites. *Compos Part A: Appl Sci Manuf* 2005; 36(11): 1525-1535.

[13] Akbari R, Beheshty M, Shervin M. Toughening of dicyandiamide-cured DGEBA-based epoxy resins by CTBN liquid rubber. *Iran Polym J* 2013; 22(5): 313-324.

[14] Ragosta G, Musto P, Scarinzi G, Mascia L, Epoxy-silica particulatenanocomposites: Chemical interactions, reinforcement and fracture toughness *Polym* 2005; 46: 10506-10516.

[15] Mirmohseni A., Zavareh S. Epoxy/acrylonitrile-butadiene-styrene copolymer/clay ternary nanocomposite as impact toughened epoxy. *J Polym Res* 2010; 17(2): 191-201.

[16] Becker O, Varley RJ, Simon GP. Thermal stability and water uptake of high performance epoxy layered silicate nanocomposites. *Eur Polym J* 2004; 40(1): 187-195.

[17] Zheng Y, Zheng Y, Ning R, Effects of nanoparticles SiO2 on the performance of nanocomposites. *Mater Let* 2003; 57(19): 2940-2944.

[18] Uddin MF, Sun CT. Improved dispersion and mechanical properties of hybrid nanocomposites. *Compos Sci Technol* 2010; 70(2): 223-230.
[19] Rostamiyan Y, Fereidoon AB. Preparation, Modeling, and optimization of mechanical properties of epoxy/HIPS/silica hybrid nanocomposite using combination of central composite design and genetic algorithm. Part 1. Study of damping and tensile strengths. *Strength Mater* 2013; 45(5): 619-634.
[20] Fereidoon A, Mashhadzadeh HA, Rostamiyan Y, Experimental, modeling and optimization study on the mechanical properties of epoxy/high-impact polystyrene/multi-walled carbon nanotube ternary nanocomposite using artificial neural network and genetic algorithm, *J Sci Eng Compos Mater* 2013; 20(3): 265-276.
[21] Rostamiyan Y, Fereidoon AB, Mashhadzadeh AH, Khalili MA. Augmenting epoxy toughness by combination of both thermoplastic and nanolayered materials and using artificial intelligence techniques for modeling and optimization. *J Polym Res* 2013; 20(6): 1-11.
[22] Mirmohseni A, Zavareh S. Modeling and optimization of a new impact-toughened epoxy nanocomposite using response surface methodology. *J Polym Res* 2011; 18(4): 509-517.
[23] Mirmohseni A, Zavareh S. Preparation and characterization of an epoxy nanocomposite toughened by a combination of thermoplastic, layered and particulate nano-fillers. *Mater Des* 2010; 31(6): 2699-2706.
[24] Leardi R. Experimental design in chemistry: A tutorial. *Analytica Chimica Acta* 2009; 652(1-2): 161-172.
[25] Zhang C, Wong WK. Optimal designs for mixture models with amount constraints. *Statistics Probability Let* 2013; 83(1): 196-202.
[26] Rostamiyan Y, Mashhadzadeh AH, Salman Khani A. Optimization of mechanical properties of epoxy-based hybrid nanocomposite: Effect of using nano silica and high-impact polystyrene by mixture design approach. *Mater Des* 2014; 56: 1068-1077.
[27] Rostamiyan Y, Fereidoon A, Ghasemi Ghalebahman A, Mashhadzadeh AH, Salmankhani A. Experimental study and optimization of damping properties of epoxy-based nanocomposite: Effect of using nanosilica and high-impact polystyrene by mixture design approach. *Mater Des* 2015; 65: 1236-1244.
[28] Rostamiyan Y, Mashhadzadeh AH, Fereidoon A. Investigation of damping and toughness properties of epoxy-based nanocomposite using different reinforcement mechanisms: Polymeric alloying, nanofiber, nanolayered, and nanoparticulate materials. *J Sci Eng Compos Mater* 2015; 22(3): 223-229.
[29] Pionteck J, Muller Y, Haubler L. Reactive epoxy-CTBN rubber blends: Reflection of changed curing mechanism in cure shrinkage and phase separation behaviour. *Macromolecular Symposia* 2011; 306-307(1): 126-140.
[30] Lopez J, Ramirez C, Abad MJ, Barral L, Cano J, Diez FJ. Blends of acrylonitrile-butadiene-styrene with an epoxy/cycloaliphatic amine resin: Phase-separation behavior and morphologies. *J ApplPolym Sci* 2002; 85(6): 1277-1286.